DOI: 10.1002/ejic.200900500

Syntheses, X-ray Diffraction Study and Characterisations of Ni and Zn Complexes of Clodronic Acid and Its Dibenzoyl Derivative

Susan Kunnas-Hiltunen,*[a] Matti Haukka,[a] Jouko Vepsäläinen,[b] and Markku Ahlgrén[a]

Keywords: Bis(phosphonate) / Clodronic dianhydrides / Nickel / Zinc / X-ray diffraction

Four new nickel and zinc bis(phosphonates) were prepared, and their crystal structures were determined by single-crystal X-ray diffractometry: $[\{Na_2Ni_3(Cl_2C(PO_2O(C(O)C_6H_5))_2)(H_2O)_{20}\}\{Cl_2C(PO_2O(C(O)C_6H_5))_2\}]_n$ (**1**), $[\{Na_2Zn_3(Cl_2C(PO_2O(C(O)C_6H_5))_2)(H_2O)_{20}\}\{Cl_2C(PO_2O(C(O)C_6H_5))_2\}]_n$ (**2**), $[Ni_2\{Cl_2C(PO_3)_2\}(H_2O)_7]\cdot 4H_2O$ (**3**) and $[Zn_2\{Cl_2C(PO_3)_2\}(H_2O)_7]\cdot 6H_2O$ (**4**). In addition, the spectroscopic and thermal properties of the compounds **1**–**4** were studied by infrared spectroscopy and thermogravimetric analysis. The coordination polymers **1** and **2** form, through intermolecular hydrogen bonds, 2D layer-like structures, whereas the aqua ligands and lattice water molecules of the monomeric compounds **3** and **4** form hydrogen bonds in three dimensions giving rise to a 3D network. In the isomorphous structures **1** and **2** the octahedral Na and Ni/Zn atoms form μ-H_2O-bridged stepped metal chains where the $Cl_2C(PO_2O(C(O)C_6H_5))_2^{2-}$ ligands (**L1**) are monodentately coordinated to the Na and Ni/Zn atoms, and the lattice **L1** ligands are located in a *trans* position with respect to the chain. The isostructural Ni and Zn complexes of clodronic acid, **3** and **4**, are formed by a hydrolysis method from the **L1** ligand. There, the clodronate ligand acts as a bridging and chelating ligand with the octahedral Ni and Zn atoms. The bulky and hydrophopic benzoyl groups of the **L1** ligand in structures **1** and **2** lead to dense packing modes. The clodronic acid ligand of structures **3** and **4**, in turn, has a higher coordination flexibility and forms voids, where the water clusters are trapped by hydrogen bonds.

Introduction

Hybrid inorganic–organic solids, especially metal phosphonates and carboxylates, have broad potential in practical applications, such as in ion exchange, catalysis and gas storage.[1] In addition, metal phosphonates and carboxylates have magnetic properties at low temperatures when the metal is paramagnetic.[1a,1c] Their structural diversity and utility in crystal engineering have been explored through the preparation of one-dimensional (1D) chains,[2] two-dimensional (2D) layers,[3] three-dimensional (3D) pillared layers[3a,4] and open framework structures.[5] The 3D networks are connected through covalent and coordinative bonds[5a–5c,6] or hydrogen bonds.[2a,5d–5e,7] In the bis(phosphonate) ligand the phosphonate groups are connected to a stable organic backbone, whereas the inorganic parts chelate or bridge the metal atoms or serve as hydrogen-bond acceptors. The observation that the dimensionality depends on the length of the organic unit, the number of donor atoms and the degree of protonation of the phosphonate groups, has guided the research on bis(phosphonate) ligands.[1a–1b] In addition, the presence of other cations, anions or neutral molecules in the starting mixture may have an effect on the dimensionality. In addition, they can act as clathrated guest molecules occupying the open cavities in crystal structures.[2a,5f–5h,8]

Accordingly, metal bis(phosphonates) can produce microporous or mesoporous materials with specifically defined cavities and high chemical and thermal stability.[1b,9] Among the space-filling molecules, small water clusters have been widely studied both theoretically and experimentally. Water is a very important factor in many biological and chemical systems, and its structural and binding properties may provide insights into the bulk properties of water. Structuring the water clusters also has an importance in the design of new metal–organic framework structures. In the case of the bis(phosphonates), water molecules are able to form four hydrogen bonds in a tetrahedral fashion, at least with water–water or water–phosphonate oxygen contacts.[10] The simplest water cluster patterns have been classified, but the hydrogen-bond networks can be extremely complex.[10a–10b]

Although bis(phosphonates), especially disodium dichloromethylenebis(phosphonate) tetrahydrate i.e. clodronate, are already clinically important drugs for the inhibition of bone resorption, their absorption in the body needs to be improved.[11] The prodrug approach is being explored for

---

[a] Department of Chemistry, University of Joensuu,
P. O. Box 111, 80101 Joensuu, Finland
Fax: +358-13-251-3390
E-mail: Susan.Kunnas-Hiltunen@joensuu.fi
[b] Department of Chemistry, University of Kuopio,
P. O. Box 1627, 70211 Kuopio, Finland

Supporting information for this article is available on the WWW under http://dx.doi.org/10.1002/ejic.200900500.

this purpose, and the clodronic dianhydrides are the first reported bioreversible prodrugs of clodronate.[12] The degree of protonation of the phosphonate groups has been modified through the addition of various ester groups, and the results, for example for metal complexes of clodronic acid derivatives, have shown that the dimensionalities of the structures decrease with decreasing protonation degree. However, 3D structures are formed when the Na^+ cation participates in structure formation.[13] The modifications of bis(phosphonates) has led to both dense and porous structures, which means that metal bis(phosphonate) structures cannot always be predicted. Therefore, our intention is to produce single crystals of diverse metal complexes of clodronic acid and its derivatives, and study their structural properties and potentiality for further research.

Recently, we reported the structures of the Mg, Sr and Ba complexes of the dibenzoyl derivative of clodronic acid: *P*,*P′*-dibenzoyl-dichloromethylenebis(phosphonate) disodium salt $Na_2Cl_2C(PO_3(COC_6H_5))_2$.[14] Our results indicated that the $Cl_2C(PO_2O(C(O)C_6H_5))_2^{2-}$ ligand (**L1**) can act as a bridging and a chelating ligand forming 2D layer structures by intermolecular hydrogen bonds between monomeric units and polymeric chains. Here, we report our preparation of isomorphic Ni and Zn complexes of the dibenzoyl derivative of clodronic acid: $[\{Na_2Ni_3(Cl_2C(PO_2O(C(O)C_6H_5))_2)(H_2O)_{20}\}\{Cl_2C(PO_2O(C(O)C_6H_5))_2\}]_n$ (**1**) and $[\{Na_2Zn_3(Cl_2C(PO_2O(C(O)C_6H_5))_2)(H_2O)_{20}\}\{Cl_2C(PO_2O(C(O)C_6H_5))_2\}]_n$ (**2**). Further, a new Ni complex of clodronic acid $[Ni_2\{Cl_2C(PO_3)_2\}(H_2O)_7]\cdot 4H_2O$ (**3**) has been synthesised by using both clodronic acid and the dibenzoyl derivative of clodronic acid, **L1**, as starting material for the ligand, and a new Zn complex of clodronic acid $[Zn_2\{Cl_2C(PO_3)_2\}(H_2O)_7]\cdot 6H_2O$ (**4**) has been prepared from the dibenzoyl derivative by a hydrolysis method. The syntheses of the complexes are presented together with the results of X-ray diffraction, IR studies and thermogravimetric analyses (TGA). In addition, the solvent-accessible void volumes were estimated for **3** and **4**.

Results and Discussion

Synthesis

The degree of protonation/deprotonation of the bis(phosphonates) is often studied by adjusting the pH of the system. In most cases, the pH determines the kind of metal bis(phosphonate) structure that forms, but it does not always affect the degree of protonation of the bis(phosphonic acid).[4b,5k] The rate of hydrolysis of the **L1** ligand is dependent on the pH,[12] but the pH changes in the same way in the formation of the alkaline earth metal complexes of **L1** and the corresponding complexes of clodronic acid.[14] The pH values of all syntheses of **1**–**4** were in the range where the ligand should not hydrolyse quickly.[12] A look at the pH of previously published[13a–13b] Zn complexes of clodronic acid and its derivatives and that of the Ni and Zn complexes **1**–**4**, shows that the Ni and Zn complexes of clodronic acid are formed at lower pH than the Ni and Zn complexes of its derivatives. In our preparation of compounds **1**–**4** we did not adjust the pH to a specific value, but the quantities of the metal salt and the **L1** ligand in the solution determined the crystallisation time and further the structure formation.

Crystal Structure of $[\{Na_2Ni_3(Cl_2C(PO_2O(C(O)C_6H_5))_2)(H_2O)_{20}\}\{Cl_2C(PO_2O(C(O)C_6H_5))_2\}]_n$ (1)

Compound **1** crystallises in space group $P\bar{1}$ and consists of polymeric chains in the direction of the crystallographic *a*-axis. The asymmetric unit contains three independent Ni and two independent Na atoms, two **L1** ligands, 20 aqua

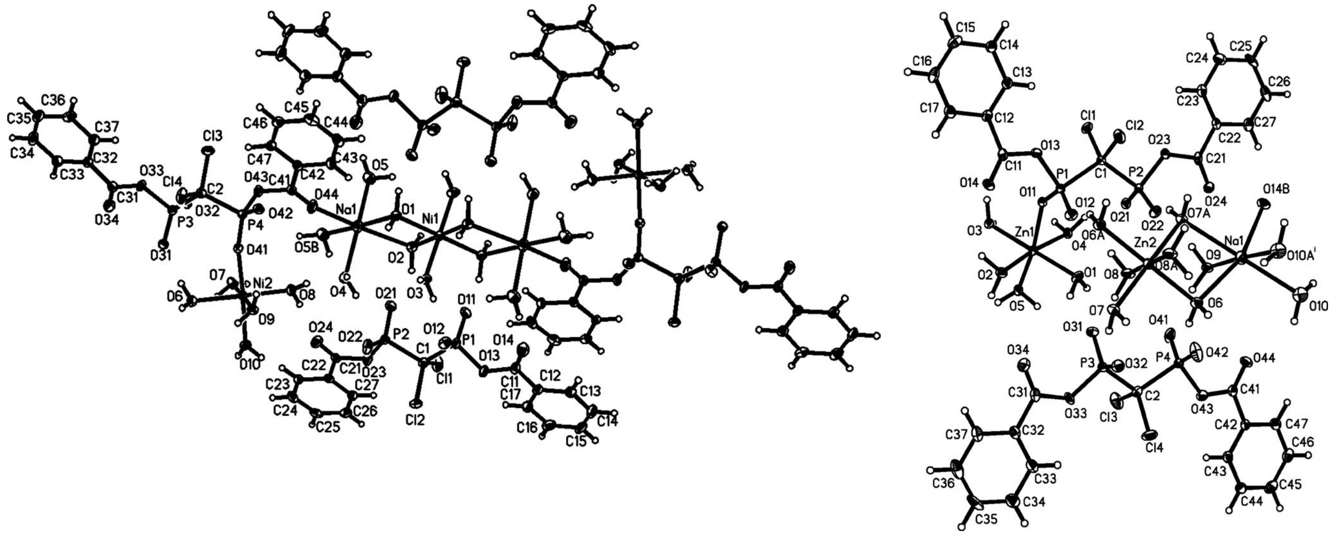

Figure 1. Part of the structures of **1** (left) and **2** (right) with thermal ellipsoids (50%) and numbering scheme. In **1**, B refers to the atom at symmetry position ($-x$, $-y + 1$, $-z$). In **2**, A refers to the atom at symmetry position ($-x$, $-y$, $-z + 1$), A^i to the atom at ($-x - 1$, $-y$, $-z + 1$) and B to the atom at ($x - 1$, y, z).

ligands and two **L1** lattice ligands (see Figure 1). The **L1** ligands are coordinated monodentately to octahedral Na1 atoms through carbonyl oxygen atoms O44 and to octahedral Ni2 atoms through phosphonate oxygen atoms O41. The other phosphonate oxygen atoms of the ligands and all phosphonate oxygen atoms of the lattice ligands are unprotonated. The octahedral Ni1 atom is located at the centre of symmetry with a site occupancy of 0.5; it bridges two Na1 atoms with four μ-H_2O ligands, and completes the coordination sphere with two aqua ligands. In addition, the

Table 1. Selected M–O bond lengths [Å] and O–M–O angles [°] for structure **1**.

Structure **1**[a]					
Ni1–O3	2.022(2)	Ni2–O9	2.098(2)		
Ni1–O1	2.062(2)	Na1–O44	2.369(2)		
Ni1–O2	2.091(2)	Na1–O5	2.402(3)		
Ni2–O8	2.028(2)	Na1–O4	2.409(3)		
Ni2–O7	2.028(2)	Na1–O2	2.439(2)		
Ni2–O41	2.038(2)	Na1–O5B	2.506(3)		
Ni2–O10	2.042(2)	Na1–O1	2.521(2)		
Ni2–O6	2.068(2)				
O3–Ni1–O3A	180.00	O7–Ni2–O10	95.02(9)	O44–Na1–O2	159.28(9)
O3–Ni1–O1A	93.64(8)	O41–Ni2–O10	169.64(9)	O5–Na1–O2	89.96(9)
O3–Ni1–O1	86.36(8)	O8–Ni2–O6	173.38(9)	O4–Na1–O2	89.95(8)
O1A–Ni1–O1	180.00	O7–Ni2–O6	85.00(8)	O44–Na1–O5A	91.64(9)
O3A–Ni1–O2	90.21(9)	O41–Ni2–O6	88.28(8)	O5–Na1–O5A	79.46(9)
O3–Ni1–O2	89.79(9)	O10–Ni2–O6	88.10(9)	O4–Na1–O5A	98.77(8)
O1A–Ni1–O2	92.62(8)	O8–Ni2–O9	93.17(9)	O2–Na1–O5A	108.55(9)
O1–Ni1–O2	87.38(8)	O7–Ni2–O9	178.07(8)	O44–Na1–O1	89.39(8)
O3A–Ni1–O2A	89.79(9)	O41–Ni2–O9	86.47(8)	O5–Na1–O1	97.75(9)
O2–Ni1–O2A	180.0	O10–Ni2–O9	84.05(9)	O4–Na1–O1	84.02(8)
O8–Ni2–O7	88.53(9)	O6–Ni2–O9	93.28(8)	O2–Na1–O1	70.66(7)
O8–Ni2–O41	93.61(8)	O44–Na1–O5	98.51(9)	O5A–Na1–O1	177.14(9)
O7–Ni2–O41	94.33(9)	O44–Na1–O4	82.20(9)		
O8–Ni2–O10	91.08(9)	O5–Na1–O4	178.09(10)		

[a] A refers to the atom at symmetry position (–*x* + 1, –*y* + 1, –*z*) and B to the atom at (–*x*, –*y* + 1, –*z*).

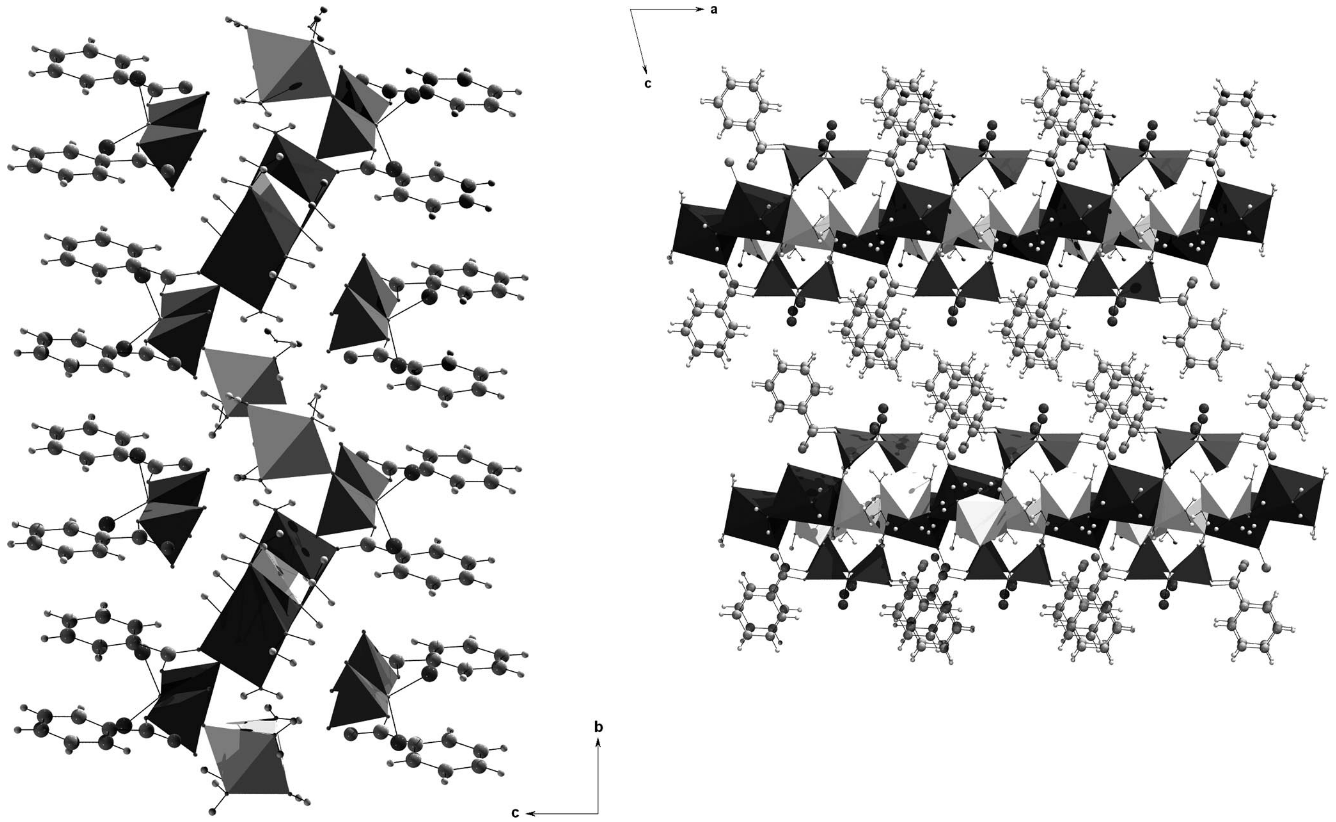

Figure 2. Polyhedral representation of structures **1** and **2**. Packing of two chains of **1** along the *a*-axis (left). Packing of **2** along the *b*-axis (right). PCO_3 tetrahedron grey, NiO_6/ZnO_6 octahedron light grey, NaO_6 octahedron dark grey.

Na1(μ-H_2O)$_2$Ni1(μ-H_2O)$_2$Na1 chains are connected to one another by two μ-H_2O oxygen atoms, O5 and O5B, forming a stepped metal chain. The remaining coordination sites of the Na1 and Ni2 atoms are occupied by aqua ligands. The Ni1–O bond lengths vary from 2.022(2) to 2.091(2) Å, the Ni2–O distances from 2.028(2) to 2.098(2) Å and the Na1–O distances from 2.369(2) to 2.521(2) Å (see Table 1). The intermetallic Ni1–Na1 distance is 3.525(1) Å, and the Na1–Na1^{iv} distance is 3.775(2) Å. A similar stair-step chain structure can be seen for example in the case of the oxidovanadium organodiphosphonate,[15] but there the adjacent chains are connected through phosphonate oxygen atoms of the $O_3P(CH_2)_3PO_3$ groups, not through μ-H_2O oxygen atoms as in structure **1**. The six-coordinate Na centres connect the adjacent chains to two- and three-dimensional structures in the Zn,[13a] Mg[13c] and Ca[13f] complexes of clodronic acid, but here the diester derivative of clodronic acid (**L1**) hinders the increase of the dimensionality. In structure **1** the Ni2 octahedron and the **L1** lattice ligands are located in a *trans* position with respect to the metal chain, which forms a 2D structure by intermolecular hydrogen bonds between the inorganic hydrophilic parts of the chains along the (001) plane. Intramolecular and intermolecular hydrogen bonds are formed between the phosphonate oxygen atoms, carbonyl oxygen atoms and aqua ligands. The intramolecular O8···O4, O2···O21, O3···O12, O6···O31, O8···O24 and O4···O22 distances are 2.676(3)–3.029(3) Å and the angles are 159–174.0°. The intermolecular O1···O11^{i}, O7···O12^{ii}, O6···O22^{iii}, O2···O42^{iv}, O4···O32^{v}, O10···O31^{vi}, O1···O32^{v}, O7···O6^{vi}, O9···O22^{iii}, O9···O34^{v}, O3···O32^{v}, O3···O42^{v}, O10···O9^{iii}, O5···O42^{iv} and O5···O14^{i} distances are 2.604(3)–3.077(3) Å (symmetry codes: i: 1 – *x*, 1 – *y*, –*z*; ii: –1 + *x*, *y*, *z*; iii: –*x*, 2 – *y*, –*z*; iv: –*x*, 1 – *y*, –*z*; v: 1 + *x*, *y*, *z*; vi: –1 – *x*, 2 – *y*, –*z*), respectively, and the angles are 128.0–176.0°. The organic hydrophobic parts of the chains lie against each other in the direction of the crystallographic *c*-axis. The packing diagram is presented in Figure 2.

Crystal Structure of [{$Na_2Zn_3(Cl_2C(PO_2O(C(O)C_6H_5))_2)(H_2O)_{20}$}{$Cl_2C(PO_2O(C(O)C_6H_5))_2$}]$_n$ (2)

Compound **2** is isomorphous with structure **1** (see Figure 1). Space group, cell dimensions and structural form are the same. The two differences are in (a) numbering and (b) the positioning of the Zn atoms. In structure **2** Zn1 occupies the position of the Ni2 atom and Zn2 the position of the Ni1 atom. The Zn1–O bond lengths range from 2.052(3) to 2.163(3) Å, the Zn2–O bond lengths from 2.048(3) to 2.153(3) Å and the Na1–O bond lengths from 2.363(2) to 2.521(3) Å (Table 2). The intermetallic Zn2–Na1 distance is 3.521(3) Å and the Na1–Na1A^{i} distance is 3.771(4) Å. The phosphonate oxygen atoms, carbonyl oxygen atoms and aqua ligands form intramolecular and intermolecular hydrogen bonds, which connect the stepped and μ-H_2O-bridged metal chains together and form a 2D layer-like structure, as in structure **1** (see Figure 2). The intramolecular O7···O32, O1···O31, O8···O31, O6···O42, O4···O21, O9···O22, O8···O12, O9···O41, O9···O42 and O8···O32 distances are 2.607(4)–3.372(4) Å and the angles are 137.0–162.0°. The intermolecular O2···O9^{i}, O4···O41^{ii}, O6···O12^{iii}, O1···O4^{ii}, O7···O22^{iii}, O5···O21^{ii}, O3···O41^{ii}, O2···O44^{i}, O3···O24^{i}, O5···O3^{iv}, O10···O12^{v}, O10···O34^{v} and O3···O44^{i} distances are 2.673(4)–3.392(5) Å (symmetry codes: i: 1 + *x*, *y*, *z*; ii: –*x*, 1 – *y*, 1–*z*; iii: –*x*, –*y*, 1 – *z*; iv: 1 – *x*, 1 – *y*, 1 – *z*; v: –1 + *x*, *y*, *z*) and the angles are 116.0–163.0°. In addition, the ligand **L1** is oriented in the packing scheme

Table 2. Selected M–O bond lengths [Å] and O–M–O angles [°] for structure **2**.

Structure **2**[a]					
Zn1–O11	2.052(3)	Zn2–O7A	2.101(3)		
Zn1–O1	2.055(3)	Zn2–O6	2.153(3)		
Zn1–O2	2.058(3)	Na1–O14B	2.363(4)		
Zn1–O5	2.091(3)	Na1–O10A^{i}	2.395(4)		
Zn1–O4	2.129(3)	Na1–O9	2.412(4)		
Zn1–O3	2.163(3)	Na1–O6	2.441(4)		
Zn2–O8	2.048(3)	Na1–O10	2.508(4)		
Zn2–O8A	2.048(3)	Na1–O7A	2.521(3)		
Zn2–O7	2.101(3)				
O11–Zn1–O1	96.22(12)	O8–Zn2–O7	93.67(12)	O14B–Na1–O10A^{i}	99.40(14)
O11–Zn1–O2	95.12(12)	O8A–Zn2–O7	86.33(12)	O14B–Na1–O9	83.14(13)
O1–Zn1–O2	89.69(13)	O8–Zn2–O7A	86.33(12)	O10A^{i}–Na1–O9	176.95(14)
O11–Zn1–O5	166.50(13)	O8A–Zn2–O7A	93.67(12)	O14B–Na1–O6	160.62(13)
O1–Zn1–O5	95.58(12)	O7–Zn2–O7A	180.0	O10A^{i}–Na1–O6	89.34(13)
O2–Zn1–O5	91.46(12)	O8–Zn2–O6	90.37(12)	O9–Na1–O6	88.75(12)
O11–Zn1–O4	87.87(12)	O8A–Zn2–O6	89.63(12)	O14B–Na1–O10	91.85(13)
O2–Zn1–O4	173.66(12)	O7–Zn2–O6	92.65(12)	O10A^{i}–Na1–O10	79.48(12)
O5–Zn1–O4	86.79(12)	O7A–Zn2–O6	87.35(12)	O9–Na1–O10	98.80(12)
O11–Zn1–O3	85.73(11)	O8–Zn2–O6A	89.63(12)	O6–Na1–O10	106.81(13)
O1–Zn1–O3	175.93(12)	O8A–Zn2–O6A	90.37(12)	O14B–Na1–O7A	88.97(12)
O2–Zn1–O3	93.70(12)	O7–Zn2–O6A	87.34(12)	O10A^{i}–Na1–O7A	98.14(12)
O5–Zn1–O3	82.09(12)	O7A–Zn2–O6A	92.66(12)	O9–Na1–O7A	83.55(11)

[a] A refers to the atom at symmetry position (–*x*, –*y*, –*z* + 1), A^{i} to the atom at (–*x* – 1, –*y*, –*z* + 1) and B to the atom at (*x* – 1, *y*, *z*).

so that the bulky organic benzyl groups lie against each other, and hydrogen bonding in that direction is not possible. Therefore, the metal complexes of the **L1** ligand form 2D structures without solvent-accessible voids.

Crystal Structure of $[Ni_2\{Cl_2C(PO_3)_2\}(H_2O)_7]\cdot4H_2O$ (3)

Compound **3** has formed by the hydrolysis crystallisation method from the dibenzoyl derivative of clodronic acid, and it crystallises in space group $P2_1/c$. The asymmetric unit consists of two independent Ni atoms, one $Cl_2C(PO_3)_2^{2-}$ ligand, seven aqua ligands and four lattice water molecules. The $Cl_2C(PO_3)_2^{2-}$ ligand both chelates and bridges two octahedral Ni atoms bidentately leaving two phosphonate oxygen atoms unprotonated. In addition, two Ni atoms are bridged by a μ-H_2O ligand (see Figure 3). This kind of bis(chelating) bonding mode is found in several structures of medronate $[H_2C(PO_3H)_2^{2-}]$,[5k,16] etidronate $[(Me)(OH)C(PO_3H)_2^{2-}]$[5c,5d] and ethylenediphosphonate $[H_4C_2(PO_3H)_2^{2-}]$.[17] The octahedral coordination spheres of Ni atoms are completed with aqua ligands having Ni1–O bond lengths of 2.026(4)–2.162(4) Å and Ni2–O bond lengths of 2.012(4)–2.152(4) Å (see Table 3). The lattice water molecules and coordinated water molecules of compound **3** form infinite hydrogen-bonded tapes along the crystallographic *b*-axis. The tapes consist of cyclic hexamers connected by two acyclic water molecules. In the hexameric ring, the lattice water oxygen atom O16 forms intermolecular hydrogen bonds to coordinated water oxygen atoms O3^{i} and O2^{i}, which furthermore form intramolecular hydrogen bonds to lattice water oxygen atoms O13 and O14, respectively. These O13 and O14 lattice water oxygen atoms form both intramolecular hydrogen bonds to the O4 μ-H_2O oxygen atom. The present cyclic hexamer possesses a chair conformation having an average O···O distance of 2.824 Å, which is longer than the corresponding value in ice I_h (2.759 Å[10c]), but can be compared to the O···O distance of liquid water (2.854 Å[10c]). The O···H···O angles vary from 96.0 to 172.0°. However, the phosphonate oxygen atoms also participate in hydrogen bonding, and they connect the tapes to a complex 3D hydrogen-bonded network (see Figure 4). In addition, intramolecular hydrogen bonds are formed between the O16···O17, O12···O14, O11···O13 and O1···O15 oxygen atoms having distances of 2.716(6)–2.856(6) Å and angles of 132.0–163.0°. The intermolecular O13···O7^{ii}, O11···O6^{ii}, O16···O15^{iii}, O15···O11^{ii}, O14···O17^{ii}, O15···O7^{iv}, O2···O9^{ii}, O1···O5^{i}, O12···O8^{v}, O13···O17^{vi},

Table 3. Selected M–O bond lengths [Å] and O–M–O angles [°] for structures **3** and **4**.

Structure **3**				Structure **4**[a]	
Ni1–O5	2.026(4)	Ni2–O9	2.012(4)	Zn1–O11	1.9917(12)
Ni1–O2	2.032(4)	Ni2–O8	2.053(4)	Zn1–O12A	2.0325(12)
Ni1–O6	2.045(4)	Ni2–O12	2.057(4)	Zn1–O4	2.0445(13)
Ni1–O3	2.071(4)	Ni2–O10	2.083(4)	Zn1–O2	2.106(2)
Ni1–O1	2.111(4)	Ni2–O11	2.088(4)	Zn1–O3	2.1165(13)
Ni1–O4	2.162(4)	Ni2–O4	2.152(4)	Zn1–O1	2.4733(12)
O5–Ni1–O2	179.2(2)	O9–Ni2–O8	95.3(2)	O11–Zn1–O12A	95.37(5)
O5–Ni1–O6	93.8(2)	O9–Ni2–O12	173.2(2)	O11–Zn1–O4	174.71(5)
O2–Ni1–O6	87.0(2)	O8–Ni2–O12	91.2(2)	O12A–Zn1–O4	89.06(5)
O5–Ni1–O3	88.7(2)	O9–Ni2–O10	90.4(2)	O11–Zn1–O2	91.64(6)
O2–Ni1–O3	90.5(2)	O8–Ni2–O10	92.9(2)	O12A–Zn1–O2	95.70(7)
O6–Ni1–O3	176.7(2)	O12–Ni2–O10	87.1(2)	O4–Zn1–O2	90.79(6)
O5–Ni1–O1	91.7(2)	O9–Ni2–O11	85.0(2)	O11–Zn1–O3	87.45(5)
O2–Ni1–O1	88.0(2)	O8–Ni2–O11	176.8(2)	O12A–Zn1–O3	173.31(5)
O6–Ni1–O1	95.4(2)	O12–Ni2–O11	88.7(2)	O4–Zn1–O3	87.85(5)
O3–Ni1–O1	86.7(2)	O10–Ni2–O11	90.3(2)	O2–Zn1–O3	90.28(7)
O5–Ni1–O4	93.0(2)	O9–Ni2–O4	94.7(2)	O11–Zn1–O1	90.14(5)
O2–Ni1–O4	87.2(2)	O8–Ni2–O4	88.1(2)	O12A–Zn1–O1	87.87(5)
O6–Ni1–O4	90.4(2)	O12–Ni2–O4	87.7(2)	O4–Zn1–O1	87.13(5)
O3–Ni1–O4	87.3(2)	O10–Ni2–O4	174.4(2)	O2–Zn1–O1	175.85(7)
O1–Ni1–O4	172.3(2)	O11–Ni2–O4	88.7(2)	O3–Zn1–O1	86.05(5)

[a] In structure **4**, A refers to the atom at symmetry position ($-x$, y, $-z + {}^1/_2$).

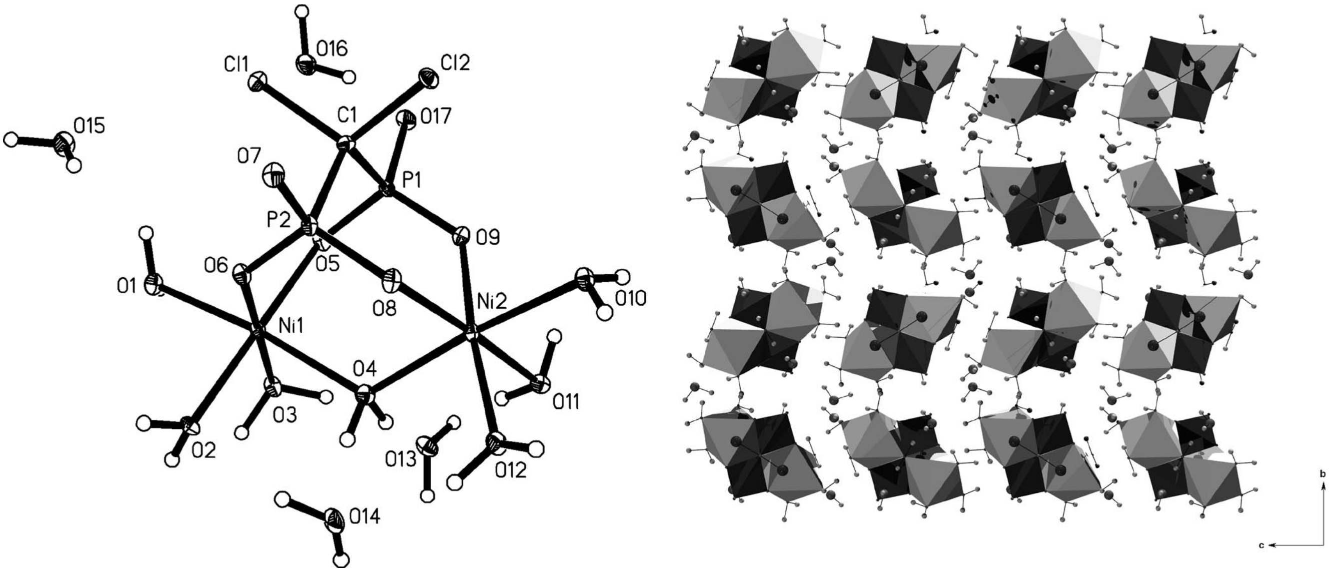

Figure 3. Structure of **3** with numbering scheme and thermal ellipsoids (50%, left) and packing of the monomeric units of **3** (right) (PCO_3 tetrahedron dark grey, NiO_6 octahedron light grey).

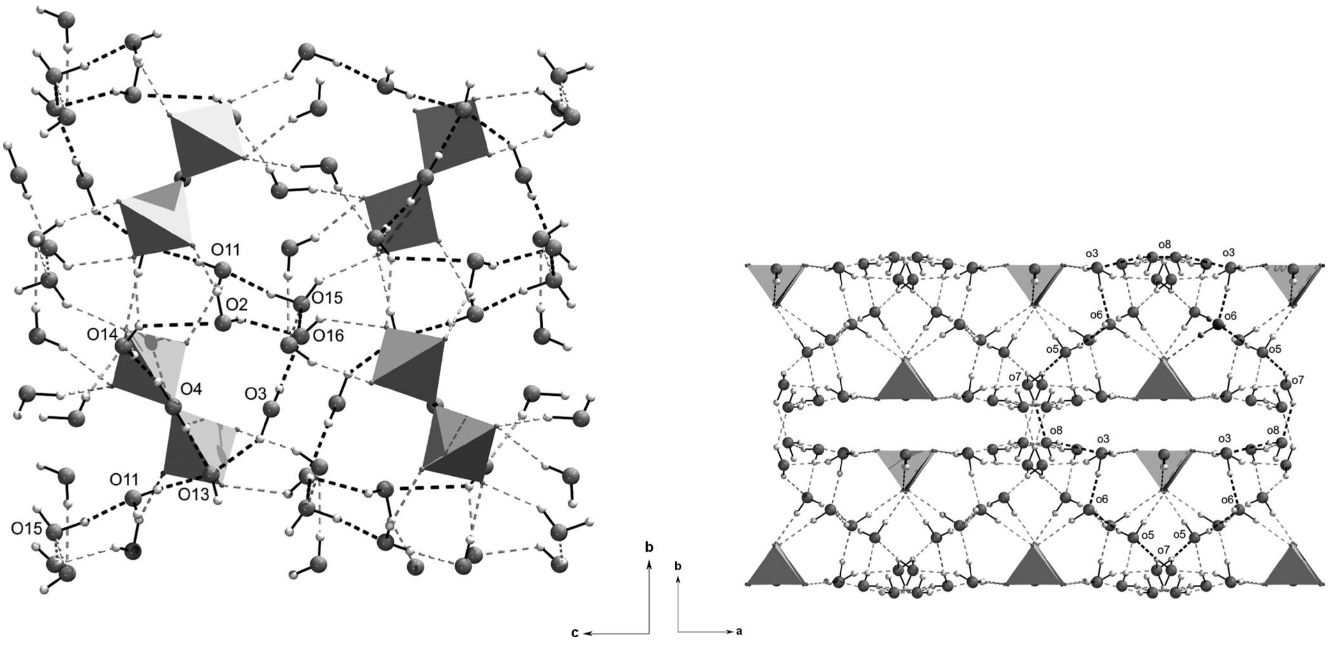

Figure 4. Close views of the hydrogen bonding of the water cluster of compound **3** (left) and compound **4** (right) (PCO_3 tetrahedron grey, oxygen atoms grey, hydrogen atoms light grey and hydrogen bond interactions grey and black dashed lines).

O10···O8^{v}, O10···O1^{ii}, O1···O3^{i} and O3···O15^{i} distances are 2.700(6)–3.158(6) Å (symmetry codes: i: –*x*, –*y*, –*z*; ii: –*x*, 0.5 + *y*, 0.5 – *z*; iii: 1 – *x*, –*y*, –*z*; iv: *x*, 0.5 – *y*, –0.5 + *z*; v: –*x*, –*y*, 1 – *z*; vi: –1 + *x*, *y*, *z*) and the angles are 120.0–177.0°. In addition, there are interactions between the O14···Cl2^{vi}, O12···Cl2^{vi}, O14···Cl1^{vi}, O3···Cl1^{vi} and O12···Cl2^{v} atoms, where the distances are 3.258(4)–3.674(4) Å, and the angles are 98.0–120.0°.

Crystal Structure of $[Zn_2\{Cl_2C(PO_3)_2\}(H_2O)_7]\cdot 6H_2O$ (4)

Compound **4** is isostructural with structure **3**, but it crystallises in space group *C*2/*c*. The asymmetric unit contains two independent and octahedral Zn atoms, one $Cl_2C(PO_3)_2^{2-}$ ligand, seven aqua ligands and six lattice water molecules. As in structure **3**, the $Cl_2C(PO_3)_2^{2-}$ ligand acts as a bridging and chelating ligand forming six- and eight-membered chelate rings with the two metal atoms (see Figure 5). The lattice water molecules O7 and O8 are disordered over two sites with equal occupancy, and the hydrogen atoms of O7 are disordered because of the twofold rotation axis. The Zn1–O bond lengths are 1.9917(12)–2.4733(12) Å (Table 3). The water cluster pattern, formed by coordinated water molecules and lattice water molecules, is three-dimensional. The polyhedral $(H_2O)_{18}$ rings surround the highly hydrophilic zinc clodronate units, and the

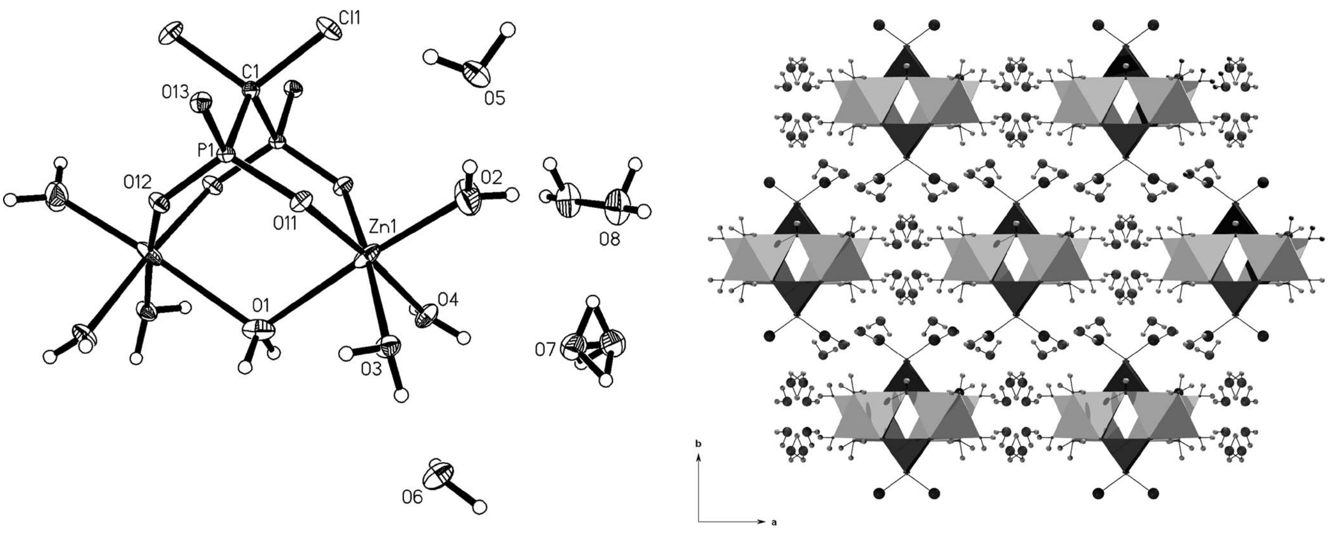

Figure 5. Structure of **4** with numbering scheme and thermal ellipsoids (50%, left) and packing of the monomeric units of **4** (right) (PCO_3 tetrahedron dark grey, ZnO_6 octahedron light grey).

phosphonate oxygen atoms complete the 3D polyhedral hydrogen-bond pattern (Figure 4). Water clusters tend to grow in size to the hexameric and higher membered water rings as the hydrophilicity of the solute molecules increases.[10d] This tendency can also be seen in structures **3** and **4**. The average O···O distance of the $(H_2O)_{18}$ ring is 2.756 Å, which is slightly shorter than the corresponding values of ice I_h (2.759 Å[10c]) and liquid water (2.854 Å[10c]). Intramolecular hydrogen bonds are formed between the aqua ligands and lattice water molecules having O2···O5, O4···O7, O7···O8, O2···O8 and O3···O6 distances of 2.713(2)–2.799(2) Å and angles of 148.7–174.0°. The O5···O13^{i}, O7···O8^{ii}, O4···O11^{iii}, O7···O5^{iv}, O3···O12^{v}, O5···O6^{vi}, O6···O6^{vii}, O2···O8^{ii}, O6···O13^{viii}, O8···O3^{iv} and O1···O13^{v}, intermolecular distances are 2.677(2)–2.912(2) Å and angles are 137.0–177.0° (symmetry codes: i: 0.5 + *x*, 0.5 – *y*, 0.5 + *z*; ii: 1 – *x*, *y*, 1.5 – *z*; iii: *x*, 1 – *y*, 0.5 + *z*; iv: 1 – *x*, 1 – *y*, 1 – *z*; v: –*x*, 1 – *y*, –*z*; vi: 0.5 – *x*, –0.5 + *y*, 0.5 – *z*; vii: 0.5 – *x*, 1.5 – *y*, 1 – *z*; viii: 0.5 – *x*, 0.5 + *y*, 0.5 – *z*).

Void Volumes

The hydrophopic and bulky benzoyl groups of the **L1** ligand in the structures **1** and **2** lead to 2D dense packing modes, and there are no lattice water molecules or solvent-accessible voids. The clodronic acid ligand is more hydrophilic, and therefore, structures **3** and **4** can form a 3D hydrogen-bond network. Significant proportions of the structures of **3** and **4** are formed by lattice water molecules between the large hydrophilic areas. All lattice water molecules in the cavities were found and refined during the structural refinement process. In addition, water clusters of compounds **3** and **4** were experimentally observed. The water of crystallisation in structures **3** and **4** was removed to determine the void spaces with the PLATON software SOLV.[18] Although originally SOLV[18] was directed to the study of organic structures, it has also proven to be a good tool to determine volumes of voids in microporous inorganic crystals.[18] Here, we are interested in the space that crystal water accommodates, even though in reality, there is a strong possibility that the crystal structure will collapse after the crystal water is removed.

Although structures **3** and **4** are isostructural, the packing modes are different, and the total potential solvent area volumes are 286.6 Å^3 for **3** and 460.0 Å^3 for **4**, and thus 16.8% of the total unit cell volume for **3** and 23.2% for **4**. These are compared with the expected volume of 40 Å^3 for a hydrogen-bonded H_2O molecule, for example. The space-filling illustrations of the solvent-accessible voids of **3** and **4** were made by the PLATON software CAVITY,[17] and they are presented in Figure 6.

Spectroscopic Properties

The characteristic IR region and bands of the ligand material **L1** and its Mg, Sr and Ba complexes have been reported earlier.[14] The assignments of the Ni and Zn complexes **1**–**4** are based on earlier results, published values for similar compounds and IR tables.[19] For compounds **1** and **2** the characteristic region was observed at 1735–700 cm^{-1}, whereas the characteristic region for the metal complexes of clodronic acid **3** and **4** appeared in the region 1135–760 cm^{-1}. The stretching frequency of O–H bonds of the water clusters in structures **3** and **4** were observed as broad

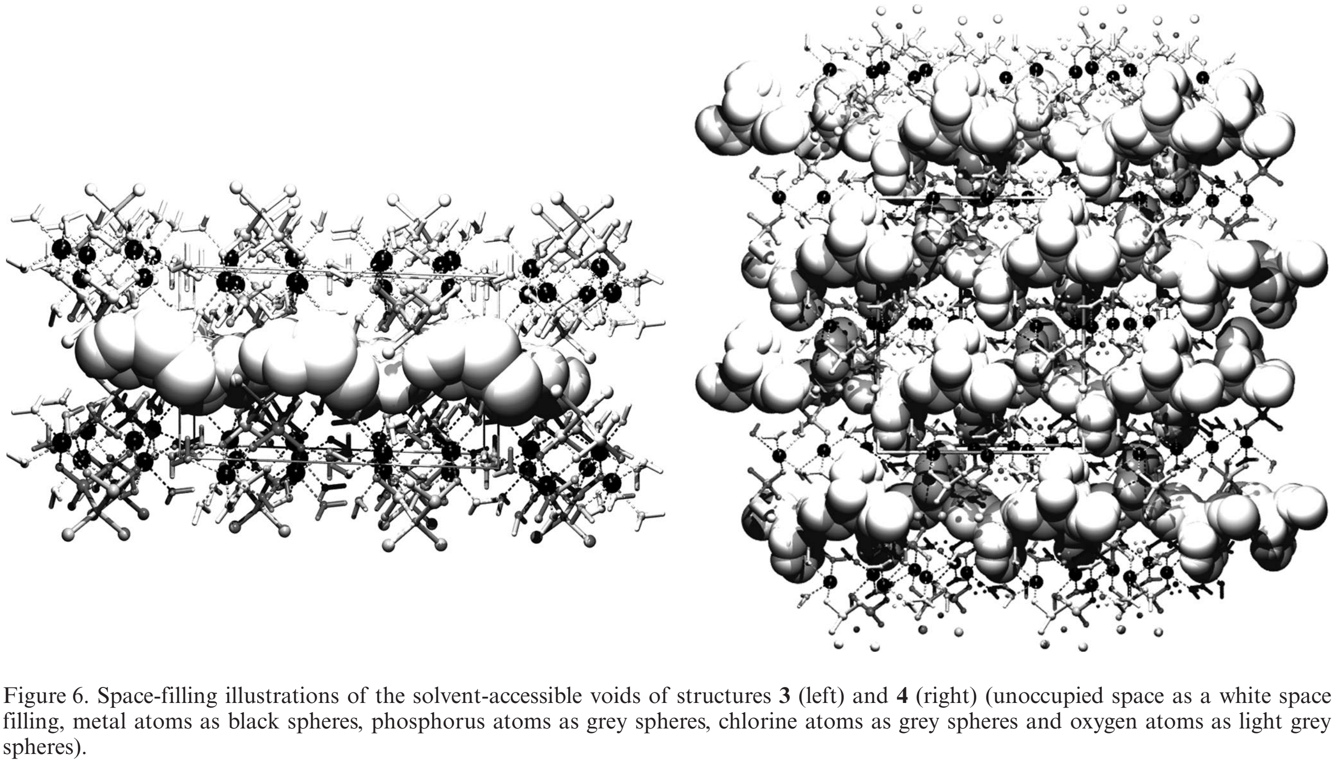

Figure 6. Space-filling illustrations of the solvent-accessible voids of structures **3** (left) and **4** (right) (unoccupied space as a white space filling, metal atoms as black spheres, phosphorus atoms as grey spheres, chlorine atoms as grey spheres and oxygen atoms as light grey spheres).

bands around 3440 cm^{-1}. The same frequencies of ice appear at 3220 cm^{-1} and of liquid water at 3490 cm^{-1} and 3280 cm^{-1}.[10c] This confirms that the O···O distances of the water clusters can be compared to liquid water O···O distances. In the spectra of structures **1** and **2** can also be seen broad bands of ν(H_2O) around 3440 cm^{-1} and weaker absorptions of δ(H–O–H) in the region of 1630 cm^{-1} due to the coordinated water molecules in the structures. The clodronic acid framework absorptions for compounds **1**–**4** were at 1330–950 cm^{-1}, attributed to the stretching vibrations of phosphonate PO_3 groups, and at 890–760 cm^{-1} attributed to the asymmetric and symmetric ν(P–C–P) vibrations. The asymmetric and symmetric ν(CCl_2) vibrations appeared at 810–680 cm^{-1}. In addition, **1** and **2** showed bands due to the benzoyl groups of the ligands. The absorptions of ν(C=O) appeared at 1740–1690 cm^{-1} with the ν(C=O) overtone at 3450 cm^{-1}, and the absorptions of ν(C–O) appeared at 1270 and 1130 cm^{-1}. The aromatic ring ν(C=C) vibrations occurred at 1605, 1588, 1495 and 1455 cm^{-1} and the stretching vibrations of the ring C–H bonds appeared as a series of bands in the 3070–2570 cm^{-1} region. The absorptions for the monosubstituted aromatic ring, due to the out-of-plane C–H vibrations, were at ca. 750 and 700 cm^{-1}.

Thermogravimetric Analyses

The TGA diagram of the starting material $Cl_2C\{PO_2O[C(O)C_6H_5]\}_2Na_2$ demonstrates two overlapping steps at about 50–800 °C attributable to the release of chlorine atoms and benzoyl groups. The black final product was multiphase, with the identifiable phase being $Na_2P_3O_{10}$. The total weight loss of 55.8% is in good agreement with the calculated value of 56.6%.

The TGA diagram for compound **1** shows three overlapping weight-loss steps at about 50–160, 160–455 and 455–900 °C attributable to the release of aqua ligands, chlorine atoms and benzoyl groups. The TGA diagram for compound **2**, in turn, shows four overlapping weight-loss steps at about 50–200, 200–455, 455–775 and 775–800 °C attributable to the release of aqua ligands, chlorine atoms, benzoyl groups and, finally, methylene carbon atoms. The total weight losses of 63.1% for **1** and 64.1% for **2** are in good agreement with the theoretical values of 62.9% and 64.4%, respectively. The identifiable phases of the final black crystalline products are $NaNi(PO_3)_3$ for **1** and $NaZn(PO_4)$ for **2**.

The TGA diagram for complex **3** exhibits three overlapping weight-loss steps at about 50–120, 120–340 and 340–800 °C attributable to the release of lattice water molecules, aqua ligands and chlorine atoms. The total weight loss of 48.6% for **3** is in good agreement with the calculated value of 48.4%. The final black product was identified to be $Ni(PO_4)$ for **3**. The loss of crystal water and coordinated water will lead to complete breakdown of the 3D lattice, since the hydrogen-bond interactions are essential for the stability of the overall structure. Definite thermogravimetric analysis of compound **4** could not be performed, since the crystals were too small, and the sample quantity was limited.

Conclusions

Two isomorphous metal complexes of an unusual derivative of clodronic acid, **1** and **2**, and two isostructural metal complexes of clodronic acid, **3** and **4**, were prepared and characterised. As a ligand, the dibenzoyl derivative of clodronic acid, **L1**, forms metal complexes with lower dimensionality than the clodronic acid, although **L1** has as many donor oxygen atoms as clodronic acid. Evidently, the spatial orientation of the phosphonate and carbonyl oxygen atoms of the **L1** ligand, the size of the organic part of the ester groups, the length of the organic chain between the phosphonate groups, and the properties of the metal are all relevant to the dimensionality. In general, the participation of the Na^+ cation in the crystal structure may increase the dimensionality and porosity. The clodronic acid metal complexes could benefit from it, but the benzoyl groups of the **L1** ligand hinder the increase of the dimensionality. In **1** and **2**, ligand **L1** is oriented in the packing scheme so that the bulky organic benzoyl groups lie against each other, and hydrogen bonding in that direction is not possible. At maximum, therefore, the **L1** ligand forms 2D structures with or without hydrogen bonding. This leads to dense packing modes without solvent-accessible voids. The clodronic acid ligand, in turn, can form a 3D hydrogen-bond network, since this ligand is more flexible and hydrophilic. In structures **3** and **4**, the lattice water molecules and the coordinated water molecules form water cluster patterns, which are trapped inside the structure through hydrogen bonding. These water clusters were observed and described, which may enhance the understanding of the properties of liquid water with a space-filling role in crystal structures. Studies on the scaling of the syntheses of structures **3** and **4** and complexing properties of other dianhydride derivatives of clodronic acid are in progress.

Experimental Section

General Procedures: All reagents used for the synthesis and characterisation of compounds **1**–**4** were of analytical reagent grade. The synthesis and characterisation of *P*,*P*′-dibenzoyl-dichloromethylenebis(phosphonate) disodium salt $Na_2Cl_2C\{PO_3[C(O)C_6H_5]\}_2$ (Na_2**L1**) have been reported earlier.[12] As has been discussed before,[14] crystallisation time is an essential factor in synthesising the metal complexes of the dibenzoyl derivative. The crystals of **L1** complexes need to form within a few days, or the hydrolysis product will form instead. In general, the crystallisation tests are carried out hydrothermally or solvothermally, but such conditions are too harsh for the derivatives of clodronic acid. The liquid crystallisation method has proved to be promising for the dianhydride ligands owing to its ease and rapidity. The gel crystallisation method, in turn, is highly effective for controlling the rate of diffusion and precipitation processes. Accordingly, compounds **1** and **2** were prepared by the liquid crystallisation method and **3** and **4** by the gel method. However, the use of compounds **1**–**4** in potential industrial applications would require scaling of the synthesis methods, which is our ongoing target. The attempt to produce powdered material of compounds **1**–**4** is challenging. The hydrolysis of the water-soluble ligand **L1** produces mixtures of metal complexes of **L1** and clodronic acid. Clodronic acid, in turn, has a high coordination flexibility of the two phosphonate groups and diverse structural properties. Therefore, it easily produces powder mixtures, as well. Thus here, we have performed all the characterisation analyses from the crystals of the additional crystallisations. Hence, compounds **1**–**4** are pure, and the crystallisation methods are reproducible. In the gel crystallisation of **3**, clodronate was dissolved in water (0.8 mL), and the solution was shaken with TMOS (0.2 mL) to form a gel. A metal salt solution (1.0 mL) was placed above the gel, and, after two weeks, was replaced by acetone (1.0 mL). In the gel crystallisation of **4**, carefully weighed amounts of **L1** and the metal salt were dissolved separately in water (2 × 0.45 mL), and the **L1** solution was warmed to 40 °C in a water bath. The solutions were mixed together, TMOS (0.1 mL) was added, and the two-phase system was shaken until homogeneous. After the gel formation, organic precipitant was added above the gel. Single crystals of **1**–**4** were selected for structural determination with a Nonius Kappa CCD diffractometer. Elemental analyses for C and H were carried out with EA 1110 CHNS-O and Carlo Erba 1106 analysers where clodronate and EDTA served as standards. The percentage values of Ni, Zn and Na were determined with a Varian 220 atomic absorption spectrophotometer. The infrared spectra were recorded with a Nicolet Magna-IR™ spectrometer 750 by the KBr pellet technique. Thermogravimetric analyses were performed with a METTLER Toledo TGA/SDTA851^e for the starting material **L1** and compounds **2** and **3** under nitrogen gas flow at a heating rate of 5 °C min^{-1} from 25 to 800 °C, and from 25 to 900 °C for compound **1**. Powder X-ray diffraction data were collected with a Bruker Avance D8 diffractometer by using Cu-K_α radiation (λ = 1.5406 Å) in the 2θ range of 5–100° with a step size of 0.05° and a counting time of 3 s per step.

$[\{Na_2Ni_3(Cl_2C(PO_2O(C(O)C_6H_5))_2)(H_2O)_{20}\}\{Cl_2C(PO_2O(C(O)C_6H_5))_2\}]_n$ (1): Water solutions of **L1** (0.030 mmol, 1 mL, pH = 3.76) and $Ni(NO_3)_2{\cdot}6H_2O$ (0.030 mmol, 1 mL, pH = 4.87) were mixed, and acetone (1 mL) was added. The solution (pH = 4.08) was allowed to stand in the cold, and green plate-like crystals were formed in 2 d (solution pH = 3.84). $C_{60}H_{80}Cl_8Na_2Ni_3O_{52}P_8$ (2386.70): calcd. C 30.19, H 3.38, Na 1.93, Ni 7.38; found C 30.16, H 3.30, Na 1.93, Ni 7.42. IR (KBr): $\tilde{\nu}$ = 1737 (m, $\nu_{C=O}$), 1602 (m, $\nu_{C=C}$), 1587 (w, $\nu_{C=C}$), 1494 (w, $\nu_{C=C}$), 1454 (m, $\nu_{C=C}$), 1270 (vs, $\nu_{P=O}$), 1179 (m, $\nu_{C–O–P}$), 1137 (m, $\nu_{C–O}$), 1108 (m, $\nu_{C–C}$), 1083 (s, $\nu_{P–O}$), 1066 (s, $\nu_{P–O}$), 1027 (m, $\nu_{P–O–C}$), 1002 (w, $\nu_{P–O–C}$), 850 (s, $\nu_{P–C–P}$), 766 (m, $\nu_{P–C–P}/\nu_{C–Cl}$), 700 (s, $\nu_{C–H}$), 680 (m, $\nu_{C–H}/\nu_{C–Cl}$) cm^{-1}.

$[\{Na_2Zn_3(Cl_2C(PO_2O(C(O)C_6H_5))_2)(H_2O)_{20}\}\{Cl_2C(PO_2O(C(O)C_6H_5))_2\}]_n$ (2): Like compound **1**, compound **2** was crystallised by the liquid crystallisation method. Water solutions of **L1** (0.089 mmol, 2.5 mL, pH = 3.74) and $Zn(NO_3)_2{\cdot}6H_2O$ (0.178 mmol, 1.0 mL, pH = 4.55) were mixed with acetone (2.0 mL). The solution (pH = 3.67) was allowed to stand in the cold, and colourless, plank-like crystals were formed over 2 d (solution pH = 3.63). $C_{60}H_{80}Cl_8Na_2O_{52}P_8Zn_3$ (2406.69): calcd. C 29.94, H 3.35, Na 1.91, Zn 8.15; found C 29.71, H 3.37, Na 1.79, Zn 7.86. IR (KBr): $\tilde{\nu}$ = 1688 (vs, $\nu_{C=O}$), 1605 (m, $\nu_{C=C}$), 1588 (m, $\nu_{C=C}$), 1497 (w, $\nu_{C=C}$), 1455 (m, $\nu_{C=C}$), 1330 (s, $\nu_{P=O}$), 1298 (s, $\nu_{C–O}$), 1190 (m, $\nu_{C–O–P}$), 1130 (m, $\nu_{C–O}$), 1103 (w, $\nu_{C–C}$), 1077 (m, $\nu_{P–O}$), 1030 (m, $\nu_{P–O–C}$), 1003 (w, $\nu_{P–O–C}$), 939 (m, $\nu_{P–C–P}$), 814 (m, $\nu_{P–C–P}$), 808 (sh, $\nu_{C–Cl}$), 712 (vs, $\nu_{C–H}$), 687 (m, $\nu_{C–Cl}$), 672 (s, $\nu_{C–H}$) cm^{-1}.

$[Ni\{Cl_2C(PO_3)_2\}(H_2O)_6]{\cdot}4H_2O$ (3): Compound **3** was prepared with either clodronate or **L1** as starting material for the ligand. In the preparation of **3** with clodronate the water solution of clodronate (0.088 mmol, 0.8 mL, pH = 3.42) was mixed with TMOS (0.2 mL). The concentrated water solution of $Ni(NO_3)_2{\cdot}6H_2O$ (0.005 mol, 1.0 mL, pH = 2.80) was placed above the gel (pH = 3.49), and after 2 weeks it was replaced with acetone (1.0 mL). Green plate-like crystals formed on the surface of the gel (pH = 1.11) within 2 weeks of the acetone addition. In the preparation of **3** with **L1** by the hydrolysis method, the water solutions of **L1** (0.0040 mmol, 0.45 mL, pH = 4.00) and $Ni(NO_3)_2{\cdot}6H_2O$ (0.0040 mmol, 0.45 mL, pH = 5.24) were mixed with TMOS (0.1 mL). After the gel (pH = 3.53) was formed, acetone was added above it, and green plate-like crystals were formed on the surface of the gel in about 1 month (pH = 2.69). $CH_{22}Cl_2Ni_2O_{17}P_2$ (556.45): calcd. C 2.16, H 3.99, Ni 21.10; found C 2.04, H 4.05, Ni 20.88. IR (KBr): $\tilde{\nu}$ = 1634 (m, $\nu_{P–O}$), 1135 (vs, $\nu_{P=O}$), 1023 (m, $\nu_{P–O}$), 975 (m, $\nu_{P–O}$), 892 (m, $\nu_{P–C–P}$), 786 (m, $\nu_{P–C–P}$), 785 (sh, $\nu_{C–Cl}$) cm^{-1}.

$[Zn_2\{Cl_2C(PO_3)_2\}(H_2O)_7]{\cdot}6H_2O$ (4): Compound **4** was formed by mixing the water solutions of **L1** (0.0100 mmol, 0.45 mL, pH = 4.00) and $Zn(NO_3)_2{\cdot}6H_2O$ (0.0200 mmol, 0.45 mL, pH = 5.20) with TMOS (0.1 mL). Acetone was added above the gel (pH = 3.40),

Table 4. Crystal data for the structures **1**–**4**.

	1	**2**	**3**	**4**
Empirical formula	$C_{60}H_{80}Cl_8Na_2Ni_3O_{52}P_8$	$C_{60}H_{80}Cl_8Na_2O_{52}P_8Zn_3$	$CH_{22}Cl_2Ni_2O_{17}P_2$	$CH_{26}Cl_2O_{19}P_2Zn_2$
Formula mass	2386.70	2406.69	556.45	605.80
T [K]	120(2)	120(2)	100(2)	150(2)
Crystal system	triclinic	triclinic	monoclinic	monoclinic
Space group	$P\bar{1}$	$P\bar{1}$	$P2_1/c$	$C2/c$
a [Å]	9.7638(2)	9.7733(2)	8.4551(11)	13.2995(2)
b [Å]	13.9400(2)	14.0285(2)	13.505(2)	16.5293(3)
c [Å]	17.2782(3)	17.2932(3)	14.9827(11)	10.3981(2)
α [°]	84.901(1)	84.745(1)	90	90
β [°]	78.984(1)	78.940(1)	91.823(7)	119.900(1)
γ [°]	79.180(1)	79.204(1)	90	90
V [Å^3]	2263.89(7)	2281.95(7)	1709.9(3)	1981.58(6)
Z	1	1	4	4
$\rho_{calcd.}$ [g cm^{-3}]	1.751	1.751	2.162	2.031
μ(Mo-K_α) [mm^{-1}]	1.108	1.268	2.782	2.935
GOF on F^2	1.015	1.054	1.178	1.036
R_{int}	0.0876	0.0793	0.0669[a]	0.0237
R_1[b] ($I \geq 2\sigma$)	0.0408	0.0439	0.0505	0.0226
wR_2[c] ($I \geq 2\sigma$)	0.0865	0.0817	0.1299	0.0556

[a] Unmerged data. [b] $R1 = \Sigma||F_o| - |F_c||/\Sigma|F_o|$. [c] $wR_2 = \{\Sigma[w(F_o^2 - F_c^2)^2]/\Sigma[w(F_o^2)^2]\}^{1/2}$.

and colourless plank-like crystals were formed on the surface of the gel (pH = 1.98) within 2 weeks. $CH_{26}Cl_2O_{19}P_2Zn_2$ (605.80): calcd. C 1.98, H 4.33, Zn 21.58; found C 2.10, H 4.16, Zn 21.85. IR (KBr): $\tilde{\nu}$ = 1634 (m, $\nu_{P–O}$), 1147 (m, $\nu_{P=O}$), 1005 (m, $\nu_{P–O}$), 934 (m, $\nu_{P–O}$), 845 (m, $\nu_{P–C–P}$), 762 (m, $\nu_{P–C–P}$), 760 (sh, $\nu_{C–Cl}$) cm^{-1}.

X-ray Crystallographic Study: X-ray diffraction data were collected with a Nonius Kappa CCD diffractometer by using Mo-K_α-radiation (λ = 0.71073 Å). Denzo and Scalepack[20] programs were used for cell refinements and data reduction. The structures were solved by direct methods with SHELXS-97,[21] and structural refinements were carried out with SHELXL-97.[21] An empirical absorption correction was applied to all of the data for **3** (TWINABS[22]) and **4** (SADABS v. 2.10[23]). Structure **3** was twinned (twin matrix [–1.000 0.000 0.000 0.000 –1.000 0.000 0.113 0.000 1.000]) and the BASF value was refined to 0.28. All H_2O hydrogen atoms of structures **1**–**4** were located from the difference Fourier map, but the O···H and H···H distances were idealised to 0.85(1) and 1.38(1) Å, respectively, and refined by using the riding model U_{iso} = 1.5. In structure **4**, water molecules O7 and O8 are disordered over two sites with equal occupancy. Furthermore, hydrogen atoms of the O7 water molecule are disordered about the twofold rotation axis. Other hydrogen atoms in structures **1** and **2** were positioned geometrically and were also constrained to ride on their parent atoms, with C–H = 0.95 Å and U_{iso} = 1.2·U_{eq} (parent atom). Crystallographic data of compounds **1**–**4** are summarised in Table 4, and selected bond lengths and angles are given in Table 5. CCDC-715322 (**1**), -715323 (**2**), -715324 (**3**) and -715325 (**4**) contain the supplementary crystallographic data for this paper. These data can be obtained free of charge from The Cambridge Crystallographic Data Centre via www.ccdc.cam.ac.uk/data_request/cif.

Table 5. Selected bond lengths [Å] and angles [°] for complexes **1**–**4**.

	1	**2**	**3**	**4**[a]
P1–O11	1.476(2)	1.481(3)		1.5214(13)
P1–O12	1.480(2)	1.477(3)		1.5199(13)
P1–O13	1.623(2)	1.627(3)		1.5139(12)
P1–O17			1.511(4)	
P1–O5			1.519(4)	
P1–O9			1.523(4)	
P2–O21	1.468(2)	1.479(3)		
P2–O22	1.484(2)	1.483(3)		
P2–O23	1.631(2)	1.641(3)		
P2–O7			1.510(4)	
P2–O6			1.519(4)	
P2–O8			1.541(4)	
P3–O32	1.482(2)	1.478(3)		
P3–O31	1.483(2)	1.482(3)		
P3–O33	1.641(2)	1.630(3)		
P4–O42	1.477(2)	1.460(3)		
P4–O41	1.481(2)	1.480(4)		
P4–O43	1.628(2)	1.628(3)		
P1–C1	1.857(3)	1.868(4)	1.866(6)	1.8617(14)
P2–C1	1.857(3)	1.855(4)	1.855(6)	
P3–C2	1.857(3)	1.852(4)		
P4–C2	1.865(3)	1.856(5)		
O11–P1–C1	108.21(13)	109.0(2)		105.03(6)
O12–P1–C1	107.98(13)	109.4(2)		104.55(6)
O13–P1–C1	97.20(12)	95.1(2)		109.10(8)
O17–P1–C1			106.6(2)	
O5–P1–C1			106.3(2)	
O9–P1–C1			103.2(2)	
O21–P2–C1	109.43(14)	109.6(2)		
O22–P2–C1	109.45(13)	108.2(2)		
O23–P2–C1	96.25(12)	96.0(2)		
O7–P2–C1			106.2(2)	
O6–P2–C1			104.5(2)	
O8–P2–C1			105.9(2)	
O32–P3–C2	107.93(13)	108.3(2)		
O31–P3–C2	109.48(13)	107.9(2)		
O33–P3–C2	96.50(12)	97.2(2)		
O42–P4–C2	109.34(13)	109.0(2)		
O41–P4–C2	108.81(13)	109.6(2)		
O43–P4–C2	95.03(12)	96.39(14)		
P1–C1–P2	111.7(2)	113.8(2)	114.1(3)	
P3–C2–P4	113.5(2)	111.9(2)		
P1A–C1–P1				113.86(13)

[a] In Structure **4** A refers to the atom at symmetry position (–*x*, *y*, –*z* + $^1/_2$).

Supporting Information (see also the footnote on the first page of this article): IR spectra for compounds **1**–**4**, TGA curves for the **L1** ligand and compounds **1**–**3** and hydrogen bond tables.

Acknowledgments

We thank Tarja Virrantalo (Dept. Chem., Univ. Joensuu) for assistance.

---

[1] a) A. Clearfield, *Progress in Inorganic Chemistry: Metal-Phosphonate Chemistry* (Ed.: K. D. Karlin), John Wiley & Sons, New York, **1998**, pp. 373–510; b) A. Clearfield, *Dalton Trans.* **2008**, 6089–6102; c) C. N. R. Rao, S. Natarajan, R. Vaidhyanathan, *Angew. Chem. Int. Ed.* **2004**, *43*, 1466–1496; d) L. Öhrström, K. Larsson, *Molecule-Based Materials – The Structural Network Approach*, Elsevier, Amsterdam, **2005**, pp. 19–38; e) K. M. Fromm, *Coord. Chem. Rev.* **2008**, *252*, 856–885.

[2] a) H.-H. Song, L.-M. Zheng, Z. Wang, C.-H. Yan, X.-Q. Xin, *Inorg. Chem.* **2001**, *40*, 5024–5029; b) R. C. Finn, R. S. Rarig, J. Zubieta Jr, *Inorg. Chem.* **2002**, *41*, 2109–2123; c) R. C. Finn, J. Zubieta, *Inorg. Chem.* **2001**, *40*, 2466–2467; d) H.-H. Song, L.-M. Zheng, C.-H. Lin, S.-L. Wang, X.-Q. Xin, S. Gao, *Chem. Mater.* **1999**, *11*, 2382–2388; e) H.-H. Song, L.-M. Zheng, G. Zhu, Z. Shi, S. Feng, S. Gao, Z. Hu, X.-Q. Xin, *J. Solid State Chem.* **2002**, *164*, 367–373; f) H.-H. Song, L.-M. Zheng, Y.-J. Liu, X.-Q. Xin, A. J. Jacobson, S. Decurtins, *J. Chem. Soc., Dalton Trans.* **2001**, 3274–3278; g) M. Dan, A. K. Cheetham, C. N. R. Rao, *Inorg. Chem.* **2006**, *45*, 8227–8238.

[3] a) D.-K. Cao, S. Gao, L.-M. Zheng, *J. Solid State Chem.* **2004**, *177*, 2311–2315; b) A. Cabeza, X. Ouyang, C. V. K. Sharma, M. A. G. Aranda, S. Bruque, A. Clearfield, *Inorg. Chem.* **2002**, *41*, 2325–2333; c) R. C. Finn, J. Zubieta, *J. Chem. Soc., Dalton Trans.* **2000**, 1821–1823; d) L.-M. Zheng, S. Gao, H.-H. Song, S. Decurtins, A. J. Jacobson, X.-Q. Xin, *Chem. Mater.* **2002**, *14*, 3143–3147; e) Z. Hulvey, D. S. Wragg, Z. Lin, R. E. Morris, A. Cheetham, *Dalton Trans.* **2009**, 1131–1135.

[4] a) Y. Gong, W. Tang, W. Hou, Z. Zha, C. Hu, *Inorg. Chem.* **2006**, *45*, 4987–4995; b) K. Barthelet, M. Nogues, D. Riou, G. Férey, *Chem. Mater.* **2002**, *14*, 4910–4918; c) N. G. Armatas, D. G. Allis, A. Prosvirin, G. Carnutu, C. J. O'Connor, K. Dunbar, J. Zubieta, *Inorg. Chem.* **2008**, *47*, 832–854; d) R. Fu, S. Hu, X. Wu, *Cryst. Growth Des.* **2007**, *7*, 1134–1144; e) K. D. Demadis, S. D. Katarachia, R. G. Raptis, H. Zhao, P. Baran, *Cryst. Growth Des.* **2006**, *6*, 836–838; f) A. Clearfield, *J. Alloys Compd.* **2006**, *418*, 128–138; g) S. Konar, J. Zon, A. V. Prosvirin, K. R. Dunbar, A. Clearfield, *Inorg. Chem.* **2007**, *46*, 5229–5236; h) C. A. Merrill, A. K. Cheetham, *Inorg. Chem.* **2007**, *46*, 278–284; i) C. A. Merrill, A. K. Cheetham, *Inorg. Chem.* **2005**, *44*, 5273–5277.

[5] a) C. Serre, G. Férey, *J. Mater. Chem.* **2002**, *12*, 2367–2369; b) Z.-G. Sun, L.-Y. Cui, Z.-M. Liu, L. Meng, H. Chen, D.-P. Dong, L.-C. Zhang, Z.-M. Zhu, W.-S. You, *Inorg. Chem. Com-*

mun. **2006**, *9*, 999–1001; c) P. Yin, L.-M. Zheng, S. Gao, X.-Q. Xin, *Chem. Commun.* **2001**, 2346–2347; d) P. Yin, Y. Peng, L.-M. Zheng, S. Gao, X.-Q. Xin, *Eur. J. Inorg. Chem.* **2003**, 726–730; e) H.-H. Song, P. Yin, L.-M. Zheng, J. D. Korp, A. J. Jacobson, S. Gao, X.-Q. Xin, *J. Chem. Soc., Dalton Trans.* **2002**, 2752–2759; f) S. Bauer, H. Müller, T. Bein, N. Stock, *Inorg. Chem.* **2005**, *44*, 9464–9470; g) H. G. Harvey, S. J. Teat, M. P. Attfield, *J. Mater. Chem.* **2000**, *10*, 2632–2633; h) C. V. K. Sharma, A. Clearfield, *J. Am. Chem. Soc.* **2000**, *122*, 4394–4402; i) A. K. Cheetham, G. Férey, T. Loiseau, *Angew. Chem. Int. Ed.* **1999**, *38*, 3268–3292; j) R. C. Finn, R. Lam, J. E. Greedan, J. Zubieta, *Inorg. Chem.* **2001**, *40*, 3745–3754; k) A. Distler, D. L. Lohse, S. C. Sevov, *J. Chem. Soc., Dalton Trans.* **1999**, 1805–1812; l) L.-M. Zheng, H.-H. Song, C.-H. Lin, S.-L. Wang, Z. Hu, Z. Yu, X.-Q. Xin, *Inorg. Chem.* **1999**, *38*, 4618–4619; m) A. Thirumurugan, P. A. Suchethan, A. K. Cheetham, C. N. R. Rao, *Z. Anorg. Allg. Chem.* **2007**, *633*, 2742–2745; n) R. K. Feller, A. K. Cheetham, *Solid State Sci.* **2006**, *8*, 1121–1125.

[6] a) J. Liang, K. H. Shimizu, *Inorg. Chem.* **2007**, *46*, 10449–10451; b) R. Fu, S. Hu, H. Zhang, L. Wang, X. Wu, *Inorg. Chem. Commun.* **2005**, *8*, 912–915.

[7] a) D.-K. Cao, Y.-Z. Li, L.-M. Zheng, *Inorg. Chem.* **2007**, *46*, 7571–7578; b) H. G. Harvey, M. P. Attfield, *Chem. Mater.* **2004**, *16*, 199–209.

[8] a) K. Barthelet, D. Riou, G. Férey, *Solid State Sci.* **2002**, *4*, 841–844; b) K. Barthelet, C. Merlier, C. Serre, M. Riou-Cavellec, D. Riou, G. Férey, *J. Mater. Chem.* **2002**, *12*, 1132–1137.

[9] a) Z. Wang, J. M. Heising, A. Clearfield, *J. Am. Chem. Soc.* **2003**, *125*, 10375–10383; b) A. Clearfield, *Chem. Mater.* **1998**, *10*, 2801–2810; c) Z. Yuan, W. Clegg, M. P. Attfield, *J. Solid State Chem.* **2006**, *179*, 1739–1749; d) M. P. Attfield, C. Mendieta-Tan, Z. Yuan, W. Clegg, *Solid State Sci.* **2008**, *10*, 1124–1131.

[10] a) L. Infantes, S. Motherwell, *CrystEngComm* **2002**, *4*, 454–461; b) L. Infantes, J. Chisholm, S. Motherwell, *CrystEngComm* **2003**, *5*, 480–486; c) D. Eisenberg, W. Kauzmann, *The Structure and Properties of Water*, Oxford University Press, Oxford, **1969**; d) K. Raghuraman, K. K. Katti, L. J. Barbour, N. Pillarsetty, C. L. Barnes, K. V. Katti, *J. Am. Chem. Soc.* **2003**, *125*, 6955–6961; e) R. Ludwig, *Angew. Chem. Int. Ed.* **2001**, *40*, 1808–1827; f) S. K. Ghosh, P. K. Bharadwaj, *Inorg. Chem.* **2004**, *43*, 6887–6889; g) S. K. Ghosh, P. K. Bharadwaj, *Eur. J. Inorg. Chem.* **2005**, 4880–4885; h) S. K. Ghosh, P. K. Bharadwaj, *Inorg. Chim. Acta* **2006**, *359*, 1685–1689; i) S. K. Ghosh, P. K. Bharadwaj, *Eur. J. Inorg. Chem.* **2006**, 1341–1344.

[11] a) J. H. Lin, *Bone* **1996**, *18*, 75–85; b) R. Hannuniemi, L. Laurén, H. Puolijoki, *Drugs Today* **1991**, *27*, 375–390.

[12] M. Ahlmark, J. Vepsäläinen, H. Taipale, R. Niemi, T. Järvinen, *J. Med. Chem.* **1998**, *42*, 1473–1476.

[13] a) M. Kontturi, E. Laurila, R. Mattsson, S. Peräniemi, J. J. Vepsäläinen, M. Ahlgrén, *Inorg. Chem.* **2005**, *44*, 2400–2406; b) M. Kontturi, S. Peräniemi, J. J. Vepsäläinen, M. Ahlgrén, *Acta Crystallogr., Sect. E* **2005**, *61*, m635–m637; c) M. Kontturi, S. Kunnas-Hiltunen, J. J. Vepsäläinen, M. Ahlgrén, *Solid State Sci.* **2006**, *8*, 1098–1102; d) M. Kontturi, E. Vuokila-Laine, S. Peräniemi, T. T. Pakkanen, J. J. Vepsäläinen, M. Ahlgrén, *J. Chem. Soc., Dalton Trans.* **2002**, 1969–1973; e) M. Kontturi, S. Peräniemi, J. J. Vepsäläinen, M. Ahlgrén, *Polyhedron* **2005**, *24*, 305–309; f) M. Kontturi, S. Peräniemi, J. J. Vepsäläinen, M. Ahlgrén, *Eur. J. Inorg. Chem.* **2004**, 2627–2631.

[14] S. Kunnas-Hiltunen, M. Matilainen, J. Vepsäläinen, M. Ahlgrén, *Polyhedron* **2009**, *28*, 200–204.

[15] V. Soghomonian, R. Diaz, R. C. Haushalter, C. J. O'Connor, J. Zubieta, *Inorg. Chem.* **1995**, *34*, 4460–4466.

[16] a) G. Bonavia, C. Haushalter, C. J. O'Connor, J. Zubieta, *Inorg. Chem.* **1996**, *35*, 5603–5612; b) J. Salta, J. Zubieta, *Inorg. Chim. Acta* **1996**, *252*, 431–434.

[17] H. G. Harvey, S. J. Teat, C. C. Tang, L. M. Cranswick, M. P. Attfield, *Inorg. Chem.* **2003**, *42*, 2428–2429.

[18] a) P. van der Sluis, A. L. Spek, *Acta Crystallogr., Sect. A* **1990**, *46*, 194–201; b) A. L. Spek, *J. Appl. Crystallogr.* **2003**, *36*, 7–13; c) H. Küppers, F. Liebau, A. L. Spek, *J. Appl. Crystallogr.* **2006**, *39*, 338–346.

[19] a) J. Kivikoski, J. M. Garcia-Ruiz, J. Vepsäläinen, F. Higes, E. Pohjala, J. Välisaari, *J. Phys. D: Appl. Phys.* **1993**, *26*, B172–B175; b) G. Socrates, *Infrared and Raman Characteristic Group Frequencies*, John Wiley & Sons, Chichester, **2001**, pp. 229–240.

[20] Z. Otwinowski, W. Minor, *Methods in Enzymology, Volume 276, Macromolecular Crystallography, Part A* (Eds.: C. W. Carter, J. Sweet), Academic Press, New York, **1997**, pp. 307–326.

[21] G. M. Sheldrick, *Acta Crystallogr., Sect. A* **2008**, *64*, 112–122.

[22] G. M. Sheldrick, *TWINABS – Bruker Nonius scaling and corrections for twinned crystals*, v. 1.05, Bruker AXS, Inc., Madison, Wisconsin, USA, **2002**.

[23] G. M. Sheldrick, *SADABS – Bruker Nonius scaling and absorption correction*, v. 2.10, Bruker AXS, Inc., Madison, Wisconsin, USA, **2003**.

Received: June 4, 2009